Multifractality and percolation in the coupling space of perceptrons

M. Weigt* and A. Engel†
Institut für Theoretische Physik, Otto-von-Guericke-Universität Magdeburg, PSF 4120, 39016 Magdeburg, Germany
(Received 20 August 1996)

The coupling space of perceptrons with continuous as well as with binary weights gets partitioned into a disordered multifractal by a set of $p=\gamma N$ random input patterns. The multifractal spectrum $f(\alpha)$ can be calculated analytically using the replica formalism. The storage capacity and the generalization behavior of the perceptron are shown to be related to properties of $f(\alpha)$ which are correctly described within the replica symmetric *Ansatz*. Replica symmetry breaking is interpreted geometrically as a transition from percolating to nonpercolating cells. The existence of empty cells gives rise to singularities in the multifractal spectrum. The analytical results for binary couplings are corroborated by numerical studies. [S1063-651X(97)11004-2]

PACS number(s): 87.10.+e, 02.50.Cw, 64.60.Ak

I. INTRODUCTION

Simple networks of formal neurons with emergent properties for information processing have been discussed within the framework of statistical mechanics for more than 10 years. In particular, the simplest case of a feed-forward neural network, the single-layer perceptron, has been analyzed from various points of view and with respect to rather different properties in numerous papers. This is mainly due to the fact that the storage as well as the generalization abilities of this network can be concisely described using the phase space formalism introduced by Gardner [1]. Part of these investigations are summarized in recent reviews [2,3].

Considering on the background of an ever-growing body of investigations aiming at more and more special aspects of this system, it seems appropriate to look for a unifying framework that allows us to characterize the various properties in a coherent fashion. In the present paper we show that the geometrical structure of the coupling space of the perceptron shattered by a random set of inputs offers such a possibility. In fact, the statistical properties of the partition of the coupling space into cells corresponding to different output sequences can be quantitatively characterized using methods from the theory of multifractals. With the help of the replica trick the multifractal spectrum can be calculated explicitly. Many of the relevant properties of the perceptron, such as the storage capacity, the typical volume of the version space, and the generalization ability, are closely related to special properties of this multifractal spectrum. As a result, the relations between different investigations become more transparent.

The idea to characterize the perceptron by the distribution of cells in coupling space induced by the inputs is rather old. It is already the basis of the classical determination of the storage capacity by Cover [4] and is frequently used in studies of information processing in mathematical statistics and computer science (see, e.g., [5]). Its qualitative appeal within the framework of statistical mechanics was emphasized by Derrida *et al.* [6] who, however, seem not to have realized that the relevant quantities could in fact be calculated. This became clear only after the work of Monasson and O'Kane [7] characterizing the distribution of internal representations in the reversed wedge perceptron. Meanwhile these investigation were extended to the case of multilayer networks and have produced several new results [8,9]. But also for the simple perceptron this formalism offers the possibility of a systematic and coherent description clarifying several delicate points of former investigations. In the present paper we present a detailed analysis of the perceptron from this point of view. Some of the results were already published in [10].

The paper is organized as follows. In Sec. II we present the general formalism of multifractals in its application to neural networks. Section III contains the analysis of the spherical perceptron, and in Sec. IV the Ising perceptron is discussed. A summary is given in the final section.

II. GENERAL FORMALISM

In this paper we are going to analyze the coupling space of simple perceptrons. These are defined by the relation

$$\sigma=\mathrm{sgn}(\mathbf{J}\cdot\boldsymbol{\xi})=\mathrm{sgn}\left(\sum_i J_i\xi_i\right) \tag{1}$$

between N input bits $\xi_i=\pm 1, i=1,\ldots,N$, and a single output $\sigma=\pm 1$. We are interested in the thermodynamic limit $N\to\infty$. The coupling vector $\mathbf{J}\in\mathbb{R}^N$ is model-dependent: For the *spherical perceptron* the only condition is the normalization of this vector to $\sqrt{N}$, in the case of the *Ising perceptron* it has binary components $J_i=\pm 1$.

We choose $p=\gamma N$ random independent and identically distributed input patterns $\boldsymbol{\xi}^\mu\in\mathbb{R}^N, \mu=1,\ldots,p$. The hyperplane orthogonal to each of these patterns cuts the coupling space into two parts according to the two possible outputs σ^μ. The p patterns therefore generate a random partition of the coupling space into 2^p (possibly empty) cells,

$$C(\{\sigma^\mu\}_{\mu=1,\ldots,p})=\{\mathbf{J};\sigma^\mu=\mathrm{sgn}(\mathbf{J}\cdot\boldsymbol{\xi}^\mu)\,\forall\,\mu\} \tag{2}$$

labeled by the 2^p output sequences $\boldsymbol{\sigma}=\{\sigma^\mu\}$ (Fig. 1).

*Electronic address: martin.weigt@physik.uni-magdeburg.de
†Electronic address: andreas.engel@physik.uni-magdeburg.de

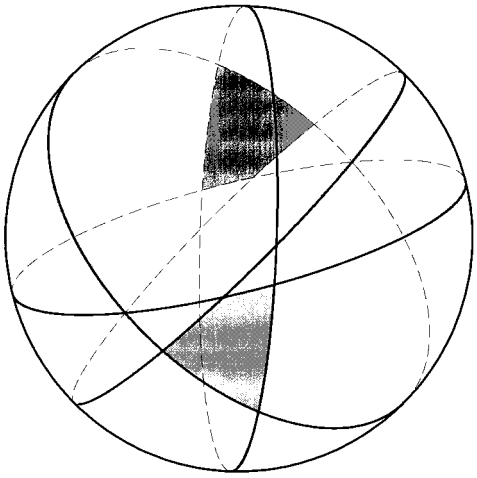

FIG. 1. Symbolic representation of the random partition of a spherical coupling space for $N=3$ and $p=4$. The figure shows the existence of a ''mirror cell'' corresponding to the symmetry of (1) under the transformation $(\mathbf{J},\boldsymbol{\sigma})\mapsto(-\mathbf{J},-\boldsymbol{\sigma})$.

The relative cell size $P(\boldsymbol{\sigma})=V(\boldsymbol{\sigma})/\Sigma_{\boldsymbol{\tau}}V(\boldsymbol{\tau})$ gives the probability for generating the output $\boldsymbol{\sigma}$ for a given input sequence $\boldsymbol{\xi}^{\mu}$ with a coupling vector $\mathbf{J}$ drawn at random from a uniform distribution over the whole space of couplings. The natural scale of this quantity in the thermodynamic limit is $\epsilon=2^{-N}$. For the Ising perceptron this corresponds to a cell containing just a single coupling vector. It is convenient to characterize the cell sizes by the *crowding index* $\alpha(\boldsymbol{\sigma})$ defined by

$$P(\boldsymbol{\sigma})=\epsilon^{\alpha(\boldsymbol{\sigma})}. \tag{3}$$

As discussed nicely in the Derrida part of [6], the storage and generalization properties of the perceptron are coded in the *distribution of cell sizes* defined by

$$f(\alpha)=\lim_{N\to\infty}\frac{1}{N\log 2}\log\sum_{\boldsymbol{\sigma}}\ \delta[\alpha-\alpha(\boldsymbol{\sigma})]. \tag{4}$$

To calculate this quantity within the framework of statistical mechanics one uses the formal analogy of $f(\alpha)$ with the microcanonical entropy of the spin system $\boldsymbol{\sigma}$ with Hamiltonian $\alpha(\boldsymbol{\sigma})$. It can hence be determined from the corresponding free energy,

$$\begin{aligned}\tau(q)&=-\lim_{N\to\infty}\frac{1}{N\log 2}\left\langle\left\langle\log\sum_{\boldsymbol{\sigma}}\ \exp(-q\log 2\,\alpha(\boldsymbol{\sigma}))\right\rangle\right\rangle\\&=-\lim_{N\to 0}\frac{1}{N\log 2}\left\langle\left\langle\log\sum_{\boldsymbol{\sigma}}\ P^{q}(\boldsymbol{\sigma})\right\rangle\right\rangle\end{aligned} \tag{5}$$

via Legendre transformation with respect to the inverse temperature q,

$$f(\alpha)=\min_{q}[\alpha q-\tau(q)]. \tag{6}$$

This procedure [10] is very similar to the so-called thermodynamic formalism in the theory of multifractals [11,12] where the multifractal spectrum $f(\alpha)$ is introduced to characterize a probability measure by the moments

$$\langle P^{q}\rangle=\sum_{\boldsymbol{\sigma}}\ P^{q}(\boldsymbol{\sigma})=\epsilon^{\tau(q)}. \tag{7}$$

In this connection $\tau(q)$ is called the *mass exponent*. The only new feature here is the additional average over the random inputs $\boldsymbol{\sigma}$ represented by $\langle\langle\cdots\rangle\rangle$ in Eq. (5). The application of multifractal techniques to the theory of neural networks was initiated by Monasson and O'Kane in their study of the distribution of internal representations of multilayer neural networks [7].

To perform the analysis for the perceptron we start with the definition of the cell size

$$P(\boldsymbol{\sigma})=\int d\mu(\mathbf{J})\prod_{\mu=1}^{p}\ \theta\left(\frac{1}{\sqrt{N}}\sigma^{\mu}\mathbf{J}\cdot\boldsymbol{\xi}^{\mu}\right) \tag{8}$$

using the Heaviside step function $\theta(x)$. The integral measure $d\mu(\mathbf{J})$ ensures that the total volume is normalized to 1.

In the thermodynamic limit we expect both τ and f to become self-averaging, and we can therefore calculate the mass exponent (5) by using the replica trick introducing n identical replicas numbered $a=1,\ldots,n$ to perform the average over the quenched patterns. Moreover, we introduce a second replica index $\alpha=1,\ldots,q$ in order to represent the qth power of P in Eq. (5) assuming as usual that the result can be meaningfully continued to real values of q [13]. Introducing integral representations for the Heaviside function we arrive at a replicated partition function given by

$$\begin{aligned}\langle\langle Z^{n}\rangle\rangle&=\left\langle\left\langle\sum_{\{\sigma_{\mu}^{a}\}}\int\prod_{a,\alpha}d\mu(\mathbf{J}^{a,\alpha})\right.\right.\\&\quad\left.\left.\times\prod_{\mu,a,\alpha}\theta\left(\sigma_{\mu}^{a}\frac{1}{\sqrt{N}}\sum_{j}\ J_{j}^{a,\alpha}\xi_{j}^{\mu}\right)\right\rangle\right\rangle\\&=\left\langle\left\langle\sum_{\{\sigma_{\mu}^{a}\}}\int\prod_{a,\alpha}d\mu(\mathbf{J}^{a,\alpha})\int_{0}^{\infty}\prod_{\mu,a,\alpha}\frac{d\lambda_{\mu}^{a,\alpha}}{\sqrt{2\pi}}\right.\right.\\&\quad\times\int\prod_{\mu,a,\alpha}\frac{dx_{\mu}^{a,\alpha}}{\sqrt{2\pi}}\exp\left\{i\sum_{\mu,a,\alpha}x_{\mu}^{a,\alpha}\left(\lambda_{\mu}^{a\alpha}\right.\right.\\&\quad\left.\left.\left.\left.-\frac{1}{\sqrt{N}}\sigma_{\mu}^{a}\sum_{i}\ J_{i}^{a\alpha}\xi_{i}^{\mu}\right)\right\}\right\rangle\right\rangle\right\rangle.\end{aligned} \tag{9}$$

The average over the quenched patterns $\boldsymbol{\xi}^{\mu}$ can now be easily done. To disentangle the remaining integrals we introduce the order parameters

$$Q_{ab}^{\alpha\beta}=\frac{1}{N}\sum_{i}\ J_{i}^{a\alpha}J_{i}^{b\beta} \tag{10}$$

as the overlap of two coupling vectors, and their conjugates $\hat{Q}_{ab}^{\alpha\beta}$. The spherical as well as the Ising constraints restrict the self-overlap $Q_{aa}^{\alpha\alpha}$ to 1. The other values of the order parameter matrices are obviously invariant under simultaneous commutations of $a\leftrightarrow b$ and $\alpha\leftrightarrow\beta$. We then find

$$\langle\langle Z^n\rangle\rangle = \int \prod_{(a,\alpha)<(b,\beta)} \frac{dQ_{a,b}^{\alpha,\beta} d\hat{Q}_{a,b}^{\alpha,\beta}}{2\pi/N} \times \exp\left\{ N\left[-\sum_{(a,\alpha)<(b,\beta)} Q_{a,b}^{\alpha,\beta}\hat{Q}_{a,b}^{\alpha,\beta} + \gamma \log G_0(Q_{a,b}^{\alpha,\beta}) + \log G_1(\hat{Q}_{a,b}^{\alpha,\beta}) \right] \right\} \tag{11}$$

with

$$G_0(Q_{ab}^{\alpha\beta}) = \int_0^\infty \prod_{a,\alpha} \frac{d\lambda^{a,\alpha}}{\sqrt{2\pi}} \int \prod_{a,\alpha} \frac{dx^{a,\alpha}}{\sqrt{2\pi}} \sum_{\{\sigma^a\}} \times \exp\left\{ i\sum_{a,\alpha} x^{a\alpha}\lambda^{a\alpha}\sigma^a - \frac{1}{2}\sum_{a,b,\alpha,\beta} x^{a\alpha}x^{b\beta}Q_{ab}^{\alpha\beta} \right\},$$

$$G_1(\hat{Q}_{a,b}^{\alpha,\beta}) = \left[\int \prod_{a,\alpha} d\mu(\mathbf{J}^{a\alpha}) \times \exp\left\{ \sum_{(a,\alpha)<(b,\beta)} \hat{Q}_{a,b}^{\alpha,\beta} \sum_i J_i^{a\alpha} J_i^{b\beta} \right\} \right]^{1/N}. \tag{12}$$

$(a,\alpha)<(b,\beta)$ denotes either $a<b$ or $a=b, \alpha<\beta$ and counts the elements above the main diagonal in the order parameter matrices. The integrals over the order parameters in Eq. (11) can be done using the saddle-point method.

To find the correct saddle point is in general a very difficult task. A simple *Ansatz* is the replica symmetric one. For the present situation it is important to note that the output sequences $\{\sigma_\mu^a\}$ carry only one replica index. The typical overlap of two coupling vectors within one cell (same output sequence $\{\sigma_\mu^a\}$) will hence in general be different from the typical overlap between two coupling vectors belonging to different cells (different output sequence $\{\sigma_\mu^a\}$). Therefore we have to introduce already within the replica symmetric (RS) approximation two different overlap values in order to determine the saddle point of Eq. (11) (see [7]):

$$Q_{ab}^{\alpha\beta} = \begin{cases} 1 & \text{if } (a,\alpha)=(b,\beta) \\ Q_1 & \text{if } a=b, \alpha\neq\beta \\ Q_0 & \text{if } a\neq b. \end{cases} \tag{13}$$

In accordance with the above discussion, Q_1 then denotes the typical overlap *within one cell*, whereas Q_0 denotes the overlap *between different cells*. The structure of the conjugated order parameter is analogous, having nonunite diagonal elements $\hat{Q}_2$.

Plugging this RS *Ansatz* into Eq. (9) one realizes that $Q_0=\hat{Q}_0=0$ always solves the saddle-point equations for Q_0 and $\hat{Q}_0$. This has an obvious physical interpretation: Due to the symmetry of Eq. (1) and therefore of the crowding index $\alpha(\boldsymbol{\sigma})$ under the transformation $(\mathbf{J},\boldsymbol{\sigma})\leftrightarrow(-\mathbf{J},-\boldsymbol{\sigma})$, every cell has a ''mirror cell'' of the same size and shape on the ''opposite side'' of the coupling space (see Fig. 1). $Q_0=0$ simply reflects this symmetry. It can be explicitly broken by introducing a threshold in Eq. (1). Note that $Q_0=\hat{Q}_0=0$ means formally that the quenched average over the input patterns can be performed as an *annealed* average.

III. THE SPHERICAL PERCEPTRON

A. Replica symmetry

In the case of the spherical perceptron the coupling space is restricted to the N-dimensional hypersphere defined by the global spherical constraint $\mathbf{J}^2=N$. In the large-N limit this gives rise to the integral measure

$$d\mu(\mathbf{J}) = \prod_i \frac{dJ_i}{\sqrt{2\pi e}} \delta(N-\mathbf{J}^2). \tag{14}$$

Using the replica symmetric *Ansatz* (13) with $Q_0=\hat{Q}_0=0$ leads to the mass exponent

$$\tau(q) = -\frac{1}{\log 2}\,\mathrm{extr}_{Q_1,\hat{Q}_{1,2}}\left[\frac{q}{2}(\hat{Q}_2-1) + \frac{q(q-1)}{2}\hat{Q}_1 Q_1 - \frac{1}{2}\log[\hat{Q}_2+(q-1)\hat{Q}_1] - \frac{q-1}{2}\log(\hat{Q}_2-\hat{Q}_1) + \gamma\log 2 \int Dt H^q\left(\sqrt{\frac{Q_1}{1-Q_1}}t \right) \right], \tag{15}$$

where we introduced the abbreviations $Dt = dt\exp(-t^2/2)/\sqrt{2\pi}$ for the Gaussian measure and $H(x)=\int_x^\infty Dt$. As is well known for spherical models, the saddle-point equations for the conjugated order parameters $\hat{Q}_{ab}^{\alpha\beta}$ can be solved explicitly, which in the present case yields

$$\tau(q) = -\frac{1}{\log 2}\,\mathrm{extr}_{Q_1}\left[\frac{1}{2}\log[1+(q-1)Q_1] + \frac{q-1}{2}\log(1-Q_1) + \gamma\log 2 \int Dt H^q\left(\sqrt{\frac{Q_1}{1-Q_1}}t \right) \right]. \tag{16}$$

The order parameter Q_1 is self-consistently determined by the saddle-point equation

$$\frac{Q_1}{1+(q-1)Q_1} = \frac{\gamma}{2\pi} \frac{\int Dt H^{q-2}\left(\sqrt{\frac{Q_1}{1-Q_1}}t \right) \exp\left\{ -\frac{Q_1}{1-Q_1}t^2 \right\}}{\int Dt H^q\left(\sqrt{\frac{Q_1}{1-Q_1}}t \right)}. \tag{17}$$

The multifractal spectrum $f(\alpha)$ resulting from a numerical solution of these equations is shown in Fig. 2 for various loadings γ.

For small values of γ we find the typical bell-shaped form of $f(\alpha)$. The zeros $\alpha_{\min}(\gamma)$ specify the RS estimate of the largest cell occurring with nonzero probability [14].

The most frequent cell size corresponds to the maximum of $f(\alpha)$ and is therefore given by $\alpha_0(\gamma)=\mathrm{argmax}(f(\alpha))$. For large N, cells of this size dominate the total number of cells exponentially, i.e., a randomly chosen *output sequence*

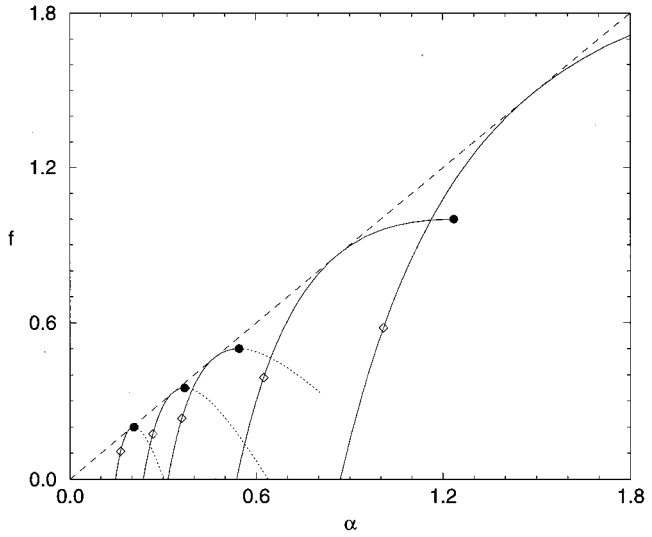

FIG. 2. Multifractal spectrum $f(\alpha)$ characterizing the cell structure of the coupling space of the spherical perceptron for various values of the loading parameter $\gamma=0.2,0.35,0.5,1.0,2.0$ (from left to right). The curves end at their maxima because of the divergence of the mass exponent $\tau(q)$ for negative q (corresponding to the dotted parts). Replica symmetry holds between the diamonds and the maxima.

$\boldsymbol{\sigma}$ will be found with probability 1 in a cell of size α_0. Hence $\epsilon^{\alpha_0(\gamma)}$ [cf. Eq. (3)] is the *typical* volume of couplings realizing $p=\gamma N$ random input-output mappings as determined within a standard Gardner calculation [1]. This volume becomes zero, i.e., $\alpha_0(\gamma)\to\infty$, for $\gamma\to 2$ (cf. Fig. 1) in accordance with the Gardner result [1].

In addition we can infer from $f(\alpha_0(\gamma))$ the *typical number* of cells as first calculated with the help of geometrical methods by Cover [4]. For small loading ratios γ we find $f(\alpha_0)=\gamma$, i.e., all $2^{\gamma N}$ possible cells (or almost all of them) do indeed occur. The storage problem for these γ values is then solvable with probability 1. For $\gamma>2$ we have $f(\alpha_0)=f(\infty)<\gamma$ implying that only an exponentially small fraction of all possible cells can be realized. It is then typically impossible to find couplings realizing a randomly generated set of input-output mappings. The multifractal analysis of the coupling space hence nicely reconciles the previously complementary approaches to the storage problem of the perceptron by Cover and Gardner, respectively. From both the analysis of $\alpha_0(\gamma)$ and of $f(\alpha_0(\gamma))$ one finds the well-known result $\alpha_c=2$.

Although the cells with volume α_0 are the most frequent ones, their joint contribution to the total *volume* of the sphere is negligible. Since

$$1=\sum_{\boldsymbol{\sigma}} P(\boldsymbol{\sigma})=\int_0^\infty d\alpha \exp\{N[f(\alpha)-\alpha]\} \tag{18}$$

a saddle-point argument reveals that the cells with size $\alpha_1(\gamma)$ defined by $f'(\alpha_1)=1$ dominate the volume. Cells of larger size are too rare, those more frequent are too small to compete. Consequently a randomly chosen *coupling vector* $\mathbf{J}$ will belong with probability 1 to a cell of size α_1. By the definition (2) of the cells all other couplings of this cell will give the same output for all patterns $\boldsymbol{\xi}^\mu$. Therefore $\epsilon^{\alpha_1(\gamma)}$ is nothing but the volume of the version space of a teacher perceptron chosen at random from a uniform probability distribution on the sphere of possible perceptrons. From it [or equivalently from $Q_1(q=1,\gamma)$] one can determine the generalization error as a function of the training set size γ reproducing the results of [15].

The main properties of the perceptron can hence be derived from the multifractal spectrum $f(\alpha)$ of the cell size distribution in the coupling space. Below we show that the RS *Ansatz* together with the assumption $Q_0=0$ gives valid results for $0\leqslant q\leqslant 1$.

There is also a close formal analogy between the calculation of $f(\alpha)$ and the standard Gardner approach with q playing the role of the replica number in the Gardner calculation. Since from Eq. (6) we have $q=df/d\alpha$, the calculation of α_0 is related to $q\to 0$, whereas the generalization problem concentrating on α_1 corresponds to $q\to 1$. These limits of the replica number in Gardner calculations are well known to correspond to the storage and generalization problems, respectively [16].

B. Longitudinal instability of replica symmetry

The results of the preceding paragraph were obtained within the RS approximation and using $Q_0=0$. The discussion of their validity requires a careful determination of the stability of these *Ansätze* for the different values of q. We first discuss the stability with respect to longitudinal fluctuations in Q_0, i.e., we search for a RS saddle-point solution where the symmetry giving rise to $Q_0=0$ is spontaneously broken. The full replica symmetric saddle-point equations are of the form

$$0=\frac{Q_0}{[1+(q-1)Q_1-Q_0]^2}-\frac{\gamma}{2\pi(1-Q_1)}\int Dy\left(\frac{\int Dt(H_+^{q-1}-H_-^{q-1})\exp\left\{-\frac{(\sqrt{Q_0}y+\sqrt{Q_1-Q_0}t)^2}{2(1-Q_1)}\right\}}{\int Dt(H_+^q+H_-^q)}\right)^2, \tag{19}$$

$$0=\frac{Q_1-Q_0}{1+(q-1)Q_1-Q_0}+\frac{Q_0(1-Q_1)}{[1+(q-1)Q_1-Q_0]^2}-\frac{\gamma}{2\pi}\int Dy\frac{\int Dt(H_+^{q-2}+H_-^{q-2})\exp\left\{-\frac{(\sqrt{Q_0}y+\sqrt{Q_1-Q_0}t)^2}{(1-Q_1)}\right\}}{\int Dt(H_+^q+H_-^q)}, \quad (20)$$

where

$$H_\pm=H\left(\pm\frac{\sqrt{Q_0}y+\sqrt{Q_1-Q_0}t}{\sqrt{1-Q_1}}\right). \quad (21)$$

Linearizing these equations in Q_0 we find that new solutions $Q_0>0$ bifurcate continuously from $Q_0=0$ at

$$q_\pm=1\pm\frac{\sqrt{\gamma}}{Q_1(\gamma)}. \quad (22)$$

From Eqs. (22) and (17) the two transition points $q_\pm(\gamma)$ for positive and negative inverse temperature q can be determined explicitly. In the range $q_-<q<q_+$, there exists only the solution with $Q_0=0$, which becomes unstable at the transition points.

C. Divergence of negative moments

The expression (15) for the replica symmetric mass exponent has been calculated for positive integer q. The continuation to negative values of q gives rise to divergences at

$$\delta=\frac{1+(q-1)Q_1}{1-Q_1}=0 \quad (23)$$

as can be realized from an asymptotic analysis of the integrand in the last term of Eq. (15). Because of $H(t)\propto\exp(-t^2/2)/\sqrt{2\pi}t$ for large t we get an exponential part of this term proportional to $\exp(-\delta t^2/2)$ and the whole integral converges only if $\delta>0$. For $\delta\to0$ we therefore find that τ tends to $-\infty$. The global minimum of Eq. (15) with respect to Q_1 is hence no longer given by the saddle point described by Eqs. (16) and (17), which realizes only a local minimum with respect to Q_1. There is hence a *discontinuous* longitudinal transition at $q=0$ with Q_1 jumping from the solution of Eq. (17) to $1/(1-q)$. As a consequence, $f(\alpha)$ is not defined for $f'(\alpha)<0$ and the curves for $f(\alpha)$ as obtained above by using the saddle-point equations are reliable only for $q\geqslant0$, i.e., for positive slope. The parts corresponding to $q<0$ are dotted in Fig. 2.

It is tempting to speculate that the observed divergence for negative q is due to the existence of *empty cells* $V(\boldsymbol{\sigma})=0$ in Eq. (5). In the theory of neural networks (and more generally of classifier systems) the possibility of output sequences impossible to implement by the system is related to the Vapnik-Chervonenkis (VC) dimension $d_{\rm VC}$ of the class of networks under consideration [18,19]. It has been notoriously difficult to determine the VC dimension of a neural network from statistical mechanics calculations since the definition of the VC dimension involves a *supremum* over all possible pattern sets rather than the *average* featuring in Eq. (5). The above analysis of the instability with respect to $Q_1,\hat{Q}_1$ for $q<0$ reveals that the multifractal formalism in the present form is unfortunately also unable to determine $d_{\rm VC}$ since the divergence of negative moments of $V(\boldsymbol{\sigma})$ occurs for *all* values of γ. The pattern average performed in Eq. (5) does not allow one to decide whether the observed divergence of τ is due to the fact that $\gamma>d_{\rm VC}/N$ or is due to exceptional pattern realizations that give rise to empty cells also if $\gamma<d_{\rm VC}/N$ [20]. Note in this connection also that similar divergences in the theory of multifractals [21] are related to cells with volume that is nonzero but decreases for $N\to\infty$ *quicker* than exponentially. For the perceptron, on the other hand, it is known that empty cells exist for all values of N [4].

D. Transversal instability of replica symmetry and percolation

In addition to the longitudinal instabilities discussed in the preceding paragraph there is the possibility of a transversal instability invalidating the RS *Ansatz* [22] which we study now. The replica symmetric *Ansatz* (13) is formally similar to a one-step replica symmetry broken solution (1RSB) of standard replica calculations [17]. It is advantageous to use the results and the notation given in [23]. After some lengthy calculations we arrive at four different eigenvalues corresponding to the replicon modes denoted by (0,1,1), (1,2,2), (0,2,2), and (0,2,1) in [23]. We give here only the result for the (0,1,1) mode which is found to be the first to become unstable,

$$\lambda(0,1,1)=\frac{1-(1/\gamma)(q-1)^2Q_1^2}{[1+(q-1)Q_1]^2}. \quad (24)$$

It vanishes exactly at the two points calculated in Eq. (22) describing the instability with respect to longitudinal Q_0 fluctuations. Similar to the SK model [24] in zero field the longitudinal and transversal instability of the RS solution occurs hence for the same temperature $1/q$ [25]. Due to the divergences for $q<0$ only q_+ is of further relevance. The AT points are therefore determined by $q_+(\gamma)$, which are marked in Fig. 2 by the diamonds.

The eigenvalue $\lambda(0,1,1)$ describes fluctuations in that part of the overlap matrix having only Q_0 entries, i.e., corresponding to the overlaps between different cells. This is reasonable since for the spherical perceptron the cells themselves are known to be convex. No RSB is hence expected to be necessary to describe the structure of a *single* cell [1]. The instability to RSB found above concerns the distribution of overlaps between different cells which must now be characterized by two parameters. The smaller one remains equal to zero reflecting still the symmetry of Eq. (1). The other one is larger than zero and describes the formation of clusters made of cells of identical size.

In order to interpret the RSB transition in physical terms we allude again to the analogy with the SK model. There the analogous instability corresponds to broken ergodicity, i.e., to the fact that not all parts of the phase space can be reached from a given initial condition. In the perceptron problem single spin flips in the output sequence $\boldsymbol{\sigma}$ are equivalent to hops between neighboring cells in the coupling space. The breakdown of $Q_0=0$ at q_+ hence signals that starting in a cell of a size corresponding to q_+, i.e., starting with a spin configuration $\boldsymbol{\sigma}$ with energy $\alpha(\boldsymbol{\sigma})$ corresponding to q_+ it becomes impossible to reach the ''mirror cell'' by hops using only cells of the same or larger sizes, i.e., via spin configurations $\boldsymbol{\sigma}$ with the same or smaller energy. Since the relative number of larger cells is exponentially small we can interpret the observed breaking of RS as a *percolation transition* in the infinite dimensional space of couplings. For $0<q<q_+$ the cells of size $\epsilon^{\alpha(q)}$ percolate in coupling space in the sense that they can all be reached from each other by entering only cells of the same size. For $q>q_+$ this is no longer true and the cells form clusters isolated from each other.

IV. THE ISING PERCEPTRON

A. Replica symmetry

In the Ising perceptron the entries of the coupling vector are restricted to $J_i=\pm 1, i=1,\ldots,N$, the full coupling space is hence given by the 2^N corners of an N-dimensional hypercube. The cells are therefore represented by discrete sets, their probability measure is given by the number of elements multiplied with 2^{-N}. Thus, the coupling space measure is to be modified according to

$$\int d\mu(\mathbf{J}) \mapsto 2^{-N}\sum_{\mathbf{J}} . \tag{25}$$

Following the general procedure described in the Sec. II we arrive at

$$\tau(q)=q+\lim_{n\to 0}\frac{1}{n\log 2}\,\mathrm{extr}_{(Q_{ab}^{\alpha\beta}),(\hat{Q}_{ab}^{\alpha\beta})}\left(\frac{1}{2}\sum_{(a\alpha)\neq(b\beta)}\hat{Q}_{ab}^{\alpha\beta}Q_{ab}^{\alpha\beta} - \log G_1((\hat{Q}_{ab}^{\alpha\beta}))-\gamma\log G_0((Q_{ab}^{\alpha\beta}))\right) \tag{26}$$

with

$$G_0((Q_{ab}^{\alpha\beta}))=\sum_{\sigma^a}\int_0^\infty\prod_{a\alpha}d\lambda^{a\alpha}\int\prod_{a\alpha}\frac{dx^{a\alpha}}{2\pi} \times\exp\left\{i\sum_{a\alpha}x^{a\alpha}\lambda^{a\alpha}\sigma^a-\frac{1}{2}\sum_{ab\alpha\beta}x^{a\alpha}x^{b\beta}Q_{ab}^{\alpha\beta}\right\} \tag{27}$$

and

$$G_1((\hat{Q}_{ab}^{\alpha\beta}))=\sum_{J^{a\alpha}}\exp\left\{\frac{1}{2}\sum_{(a\alpha)\neq(b\beta)}\hat{Q}_{ab}^{\alpha\beta}J^{a\alpha}J^{b\beta}\right\}. \tag{28}$$

Contrary to the spherical case, the conjugated parameters $\hat{Q}^{\alpha\beta}$ cannot be eliminated analytically. The replica symmetric expressions are obtained by introducing the saddle-point structure (13) for both the overlaps and their conjugates. Starting again with the solution $Q_0=\hat{Q}_0=0$ we get for the mass exponent

$$\tau(q)=\frac{1}{\log 2}\,\mathrm{extr}_{Q_1,\hat{Q}_1}\left[\frac{q\hat{Q}_1}{2}[1+(q-1)Q_1] -\log\int Dt\cosh^q(\sqrt{\hat{Q}_1}t) -\gamma\log 2\int DtH^q\left(\sqrt{\frac{Q_1}{1-Q_1}}t\right)\right]. \tag{29}$$

The extremization in this equation is again somewhat subtle [9]. There are two, qualitatively different possibilities. (i) The first one is given by $Q_1=1$ and $\hat{Q}_1=\infty$ and hence lies at the boundary of allowed values of the saddle-point parameters. It can be studied analytically and leads to $\tau(q)=q-1$. The corresponding multifractal spectrum is given by a single point $f=\alpha=1$. No dependence on γ remains. The value $\alpha=1$ describes cells containing just a single coupling vector in accordance with $Q_1=1$. Their total number is of order $\epsilon^{-f}=2^N$, and hence they form a macroscopic part of the cell number as well as of the total coupling space volume. Since the total number of cells is $2^{\gamma N}$, this solution can exist for $\gamma\geqslant 1$ only. (ii) The second solution solves the saddle-point equations

$$Q_1=\frac{\int Dt\cosh^{q-2}(\sqrt{\hat{Q}_1}t)\sinh^2(\sqrt{\hat{Q}_1}t)}{\int Dt\cosh^q(\sqrt{\hat{Q}_1}t)},$$

$$\hat{Q}_1=\frac{\gamma}{2\pi(1-Q_1)}\,\frac{\int dt\exp\left\{-\frac{(1+Q_1)t^2}{2(1-Q_1)}\right\}H^{q-2}\left(\sqrt{\frac{Q_1}{1-Q_1}}t\right)}{\int DtH^q\left(\sqrt{\frac{Q_1}{1-Q_1}}t\right)}. \tag{30}$$

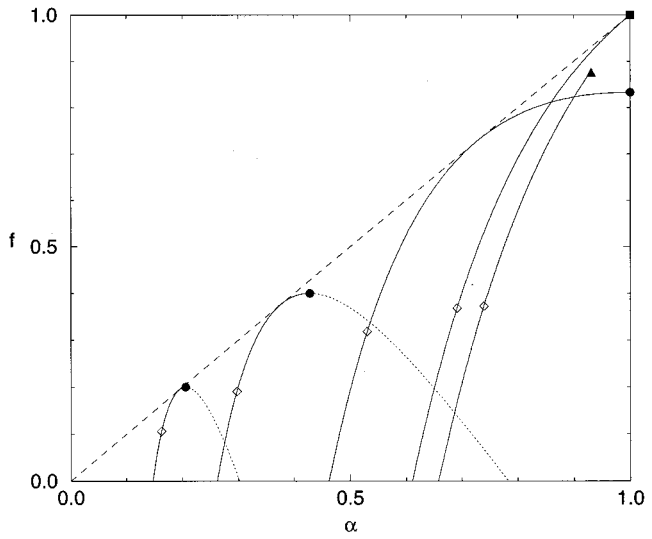

FIG. 3. Multifractal spectrum $f(\alpha)$ describing the cell structure of the coupling space of the Ising perceptron with loading ratios $\gamma=0.2,0.4,0.833,1.245,1.4$ (from left to right). The curves end at their maxima due to the divergence of the mass exponent $\tau(q)$ for negative q. Between the diamonds and the maxima RS holds. The triangle denotes the discontinuous transition to $Q_1=1$. The isolated point (1,1) is marked by the square.

It lies inside the intervals for the parameters and is to be determined numerically. It exists for all q if $\gamma\leqslant 1$ and disappears for fixed $\gamma>1$ at a sufficiently negative q.

A numerical comparison of the corresponding local maxima or minima of τ leads to the following scenario: For $\gamma<1$ solution (ii) always gives the global extremum. For $\gamma>1$ this is only the case for $q>q_{\rm disc}(\gamma)$. At this threshold the extremum (i) becomes the global one by a discontinuous transition. The occurrence of such transitions is the trademark of neural networks with Ising couplings [26,9]. The smooth curves of $f(\alpha)$ then terminate and are completed by a single point at (1,1) (see Fig. 3). Hence for $\gamma>1$ the spectrum is nonzero only in a certain region $\alpha_{\rm min}<\alpha<\alpha_{\rm max}<1$ and at the isolated point at $\alpha=1$.

The general form of the multifractal spectrum resembles that of the spherical perceptron. In fact, for $\gamma\lesssim 0.25$ the curves almost coincide. This was to be expected because the cells are still relatively large and do not ''sense'' the discreteness of the Ising couplings. For larger γ, however, it becomes decisive that in the Ising perceptron the cell sizes are restricted to $\alpha\leqslant 1$. All values $\alpha>1$ correspond to empty cells.

The storage capacity is therefore not given by $\alpha_0\to\infty$ as in the case of the spherical perceptron but is determined by $\alpha_0(\gamma)=\ \mathrm{argmax}(f(\alpha,\gamma))=1$. As can be seen from Fig. 3, this holds for $\gamma_c=0.833$ the well known result obtained in [26]. In fact, $\alpha_0(\gamma)=1$ is equivalent to the zero-entropy condition frequently used for neural networks with discrete couplings. Let us define the entropy

$$s=\lim_{N\to\infty}\frac{1}{N}\langle\langle\log\mathcal{N}\rangle\rangle, \tag{31}$$

where $\mathcal{N}$ denotes the number of couplings that can implement a mapping between γN random inputs *and* outputs. Therefore $\mathcal{N}$ is related to the size of the typical cell and from Eqs. (8) and (25) one finds $s=(1-\alpha_0)\log 2$. Hence $s=0$ is equivalent to $\alpha_0=1$.

Similarly the generalization behavior of the Ising perceptron differs from that of the spherical one. There is a well-known *discontinuous transition to perfect generalization* at $\gamma_g=1.245$ [27]. It shows up in the multifractal spectrum $f(\alpha,\gamma)$ as the point where $\alpha_1(\gamma_g)=1$ with α_1 again defined by $f'(\alpha_1)=1$. At this value of the loading parameter the discontinuous transition to $Q_1=1$ occurs and the coupling space becomes dominated by cells with exactly one element. This is the intuitive reason for the transition to perfect generalization; there is only one coupling vector left that performs perfectly on the training set: the teacher herself.

B. Continuous replica symmetry breaking and percolation

Similar to Sec. II, we have analyzed the longitudinal and transversal stability of the RS solution with $Q_0=\hat{Q}_0=0$ by calculating the relevant eigenvalues of the fluctuation matrix. The results are qualitatively the same. Using the linearization of the complete replica symmetric saddle point equations at $Q_0=\hat{Q}_0=0$ we find again a new solution with $Q_0,\hat{Q}_0>0$ emerging continuously at the two values $q_\pm$ satisfying

$$\sqrt{\gamma}=\pm\hat{Q}_1(q_\pm-1)(1-Q_1)[1+(q_\pm-1)Q_1]. \tag{32}$$

The analysis of the transversal fluctuations reveals that the first mode to become unstable is again the replicon mode (0,1,1). Due to the existence of two order parameter matrices the analysis is now more involved. Following the argumentation in [1], we first determine the eigenvalues in the two building blocks of the fluctuation matrix and find for the (0,1,1) eigenvalue of the overlap fluctuations

$$\lambda^{(Q)}(0,1,1)=-\gamma^{-1}(q-1)^2(1-Q_1)^2\hat{Q}_1^2, \tag{33}$$

and for the conjugated matrix

$$\lambda^{(\hat{Q})}(0,1,1)=-[1+(q-1)Q_1]^2. \tag{34}$$

The total fluctuation matrix for this replicon mode is then given by

$$\begin{pmatrix}\lambda^{(Q)}(0,1,1) & 1\\ 1 & \lambda^{(\hat{Q})}(0,1,1)\end{pmatrix} \tag{35}$$

and the breakdown of RS is signaled by a change of the sign of its determinant. From Eqs. (33), (34), and (35) we find that the local transversal instability occurs again at the same values $q_\pm(\gamma)$ given by Eq. (32), for which the RS solution with $Q_0=\hat{Q}_0=0$ becomes longitudinally unstable.

In Fig. 3 the breakdown of the local stability of RS is again marked by the diamonds. Inside the interval $(\alpha(q_+),\alpha_0)$, RS is locally stable. As discussed already for the spherical case, in this region the solutions are symmetric under the reflection symmetry of the original system (1) and the cells of every fixed crowding index $\alpha\in(\alpha(q_+),\alpha_0)$ percolate in coupling space. Outside this interval the overlaps between different cells must again be described by two (or more) order parameters. The smaller one vanishes, and still

reflects the symmetry of Eq. (1). The other one takes a value in $(0,Q_1)$ with Q_1 being the overlap within one single cell and describes the size of the connected clusters remaining below the percolation threshold.

C. Divergence of negative moments

For $q<0$ there occurs an analogous divergence of τ for small δ defined by Eq. (23) as in the spherical case, which gives rise to a similar discontinuous transition with respect to Q_1. As a result, the $f(\alpha)$ curves do not continue into regions of negative slope for *any* γ. It is hence again impossible to infer the (still unknown [28]) VC dimension of the Ising perceptron from the multifractal analysis. Note that the only value that could in principle be obtained from a statistical mechanics analysis is what is called the *typical* VC dimension that gives the maximal pattern set size for which *typically* no empty cells occur [29]. Numerical investigations suggest that this value is equal to $N/2$ [30,29].

D. Discontinuous replica symmetry breaking

Contrary to the case of the spherical perceptron, there is an inconsistency even within the region of *local* stability of the RS *Ansatz*. For $0.833<\gamma<1.245$ the multifractal spectrum $f(\alpha)$ continues to values $\alpha>1$ corresponding to the unphysical region of cells having less than one but more than zero elements.

We therefore expect a discontinuous transition to RSB already in the region of local stability of RS. Due to the fact that a single cell is not necessarily connected for the Ising perceptron, this transition is likely to take place inside the blocks describing the overlaps *within a cell*. The global reflection symmetry remains unbroken and therefore the typical overlaps between two cells stay zero. We can hence calculate the annealed average $\langle\langle Z\rangle\rangle$ of the partition function. After a standard calculation we find the following one-step RSB (1RSB) result for the mass exponent:

$$\begin{aligned}\tau^{\mathrm{1RSB}}(q)=\frac{1}{\log 2}\,\mathrm{extr}_{m,Q_1,Q_2,\hat{Q}_1,\hat{Q}_2}\Bigg\{&\frac{1}{2}q(q-m)Q_1\hat{Q}_1\\&+\frac{q}{2}\hat{Q}_2[1+(m-1)Q_2]-\log\int Dz_1\\&\times\Bigg[\int Dz_2\cosh^m\!\left(\sqrt{\hat{Q}_1}z_1+\sqrt{\hat{Q}_1-\hat{Q}_2}z_2\right)\Bigg]^{q/m}\\&-\gamma\log 2\int Dt_1\int Dt_2 H^m\\&\times\left(\frac{\sqrt{Q_1}t_1+\sqrt{Q_2-Q_1}}{\sqrt{1-Q_2}}\right)\Bigg]^{q/m},\end{aligned}\tag{36}$$

where Q_2 is the order parameter inside the $m\times m$ diagonal blocks of the overlap matrix and Q_1 is the entry outside these blocks. $\hat{Q}_{1,2}$ are the corresponding conjugated quantities. A similar expression was obtained in [9].

Guided by previous experience [26], we look for an extremum with $Q_2=1$ and $\hat{Q}_2=\infty$. One then finds

$$\tau^{\mathrm{1RSB}}(q)=\mathrm{extr}_m\left[q\left(1-\frac{1}{m}\right)+\tau^{\mathrm{RS}}\left(\frac{q}{m}\right)\right],\tag{37}$$

where we have used the RS mass exponent τ^{RS} from Eq. (29). The saddle-point equation with respect to m is then given by

$$1=\frac{d\tau^{\mathrm{RS}}}{dq}\left(\frac{q}{m}\right)=\alpha^{\mathrm{RS}}.\tag{38}$$

Comparing the values of τ^{RS} and τ^{1RSB}, one finds that for $\gamma>0.833$ there is indeed a *discontinuous transition* to this 1RSB solution when α gets larger than 1. Crossing this point $\tau(q)$ becomes proportional to q, implying that $f(\alpha)$ stops at $\alpha=1$. This removes the inconsistency noted above. For $0.833<\gamma<1.245$ the cells contributing most to the total volume (the α_1 cells) contain exponentially many couplings. The majority of cells, however, comprise only subexponentially many couplings. This situation is correctly described by the 1RSB solution with $Q_1<1$ characterizing the α_1 cells and $Q_2=1$ characterizing the typical ones. With increasing γ, the α_1 cells shrink and the typical cells disappear. At $\gamma=1.245$, we have $\alpha_1=1$ and correspondingly $Q_1=1$. At this point τ is again given by the *minimum* in Eq. (26) since $q>1$. Therefore the 1RSB solution has to be rejected and the discontinuous transition disappears. The 1RSB solution also becomes intrinsically inconsistent since there is ''no room left'' for a Q_2 with $Q_1<Q_2\leqslant 1$. For $\gamma>1.245$ the 1RSB solution finds its natural continuation in the RS solution with $Q_1=1$, which gives rise to the gap in the $f(\alpha)$ spectrum as discussed in the first paragraph of this section.

E. Numerical results

For the Ising perceptron the phase space is discrete and the analytical results discussed above can be checked by numerical enumerations over all the possible 2^N coupling vectors $J_i=\pm 1$. Although these techniques are naturally confined to rather low values of N, it is interesting to see whether the asymptotic behavior already shows up in small samples. We have performed enumerations for values of N between 10 and 30 according to the following prescription. We first generate p patterns at random from a Gaussian distribution with zero mean and unit variance. As in related studies [31,6] we choose Gaussian patterns because they show less pronounced finite size fluctuations. Next we use the GRAY code [32] to run through all coupling vectors **J** and determine the corresponding output strings. Finally we determine the size of the cells by counting the multiplicity of the occurring outputs and compile a histogram of cell sizes in a double logarithmic scale. The results are averaged over 10^4 (for $N=10$) to 10 (for $N=30$) realizations of the random patterns. Although the main reason for the lesser number of realizations used for large N was limited computer time, it became quite clear in the simulations that the sample-to-sample fluctuations for large N are due to self-averaging substantially smaller than for small N. The results of the enumerations together with the corresponding analytical results already displayed in Fig. 3 are shown in Fig. 4. It is at first surprising that the histograms lie always above the analytical curves. However, for small γ we have

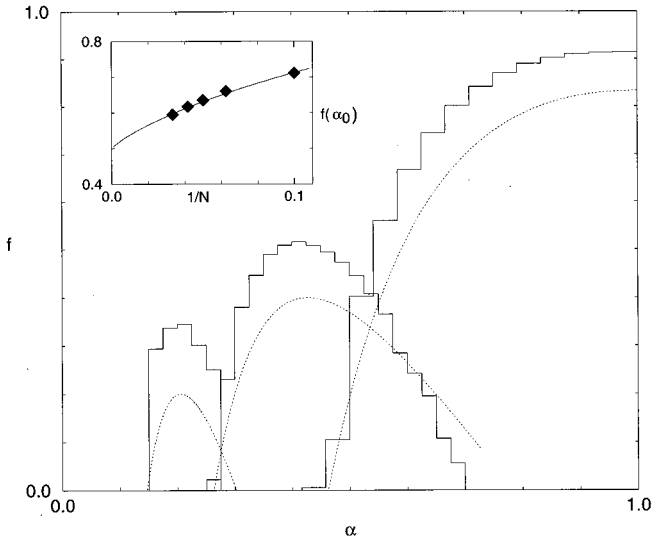

FIG. 4. Exact enumeration results for the multifractal spectrum $f(\alpha)$ of the Ising perceptron for $p=6, N=30$; $p=12, N=30$; and $p=20, N=24$ (from left to right). The dotted lines are the analytical results of Fig. 3 for $\gamma=0.2$, 0.4, and 0.833, respectively. The inset shows a finite size scaling for $f(\alpha_0)$ at $\gamma=0.5$. The diamonds are enumeration results whereas the line is given by Eq. (40) with $|f''(\alpha_0)|$ estimated from the numerical data. The rms fluctuations of the enumeration results are smaller than the symbol size. The asymptotic value for $f(\alpha_0)$ is 0.5.

$$2s^{\gamma N}=\int_0^1 d\alpha 2^{Nf(\alpha)}\simeq 2^{Nf(\alpha_0)}\int_0^1 d\alpha \exp\left(\frac{N}{2}\log 2\, f''(\alpha_0)(\alpha-\alpha_0)^2\right)\simeq 2^{Nf(\alpha_0)}\sqrt{\frac{2\pi}{N\log 2|f''(\alpha_0)|}} \tag{39}$$

giving rise to

$$f(\alpha_0)=\gamma+\frac{1}{2N}\log\frac{N\log 2|f''(\alpha_0)|}{2\pi}. \tag{40}$$

Hence the maximum of the histograms for finite N converges to the asymptotic value $f(\alpha_0)=\gamma$ for $N\to\infty$ from above. In fact, in the inset of Fig. 4 we have compared the finite size scaling predicted by Eq. (40) with enumeration results for $f(\alpha_0)$ at $\gamma=0.5$. The agreement is very good.

V. SUMMARY

In this paper, we have presented a multifractal analysis of the coupling space of the single-layer perceptron with continuous and Ising couplings. This has been done by characterizing the random partition of the coupling space into different cells corresponding to different output sequences on the same fixed set of random input vectors. This picture allowed us to refine the standard Gardner analysis and, moreover, to unify the different approaches to the storage problem of Gardner [1] and Cover [4] and the generalization problem within one consistent picture. The different questions are related to different fractal subsets of the coupling space: The cells with the most frequent size describe the storage problem, those dominating the total volume are related to the generalization ability for a randomly drawn teacher.

We have shown that the storage and the generalization problem can always be analyzed within the region where replica symmetry is locally stable. Moreover we have demonstrated that the most important part of the multifractal spectrum can be determined within an annealed calculation with respect to the input pattern distribution. This is not only an important technical advantage but may also smooth the way for mathematically rigorous investigations of these problems.

Replica symmetry must be broken if one aims at describing comparatively large and therefore rare cells. Despite the symmetry of the coupling space under point reflection at the origin, these cells no longer percolate in the sense that it is impossible to reach the corresponding ''mirror'' cell without entering cells of smaller size. This clustering of large cells is described by the higher order parameters of a solution with broken replica symmetry.

Finally we note that the central procedure in our calculations is the determination of *positive integer* moments V^q of the distribution of phase space volumes and the continuation of the result to real q [13]. In doing so we encountered divergences for all $q<0$. These are probably due to the existence of empty cells $V=0$. We therefore hope that an appropriately modified formalism describing the metastable state that occurs for $q<0$ might be able to yield also results for the VC dimension of neural networks.

ACKNOWLEDGMENTS

Stimulating discussions with Rémi Monasson and Tamás Tél are gratefully acknowledged.

[1] E. Gardner, J. Phys. A **21**, 257 (1988); E. Gardner and B. Derrida, *ibid.* **A21**, 271 (1988).
[2] M. Opper and W. Kinzel, in *Models of Neural Networks III*, edited by E. Domany, J. L. van Hemmen, and K. Schulten (Springer, New York, 1996).
[3] T. L. M. Watkin, A. Rau, and M. Biehl, Rev. Mod. Phys. **65**, 499 (1993).
[4] T. M. Cover, IEEE Trans. Electron. Comput. **EC-14**, 326 (1965).
[5] D. Haussler, M. Kearns, and R. Schapire, *Bounds on the Sample Complexity of Bayesian Learning Using Information Theory and the VC Dimension, Proceedings of the Conference on Computional Learning Theories '91* (Morgan Kaufmann, San Mateo, 1991).
[6] B. Derrida, R. B. Griffith, and A. Prügel-Bennett, J. Phys. A **24**, 4907 (1991).
[7] R. Monasson and D. O'Kane, Europhys. Lett. **27**, 85 (1994).
[8] R. Monasson and R. Zecchina, Phys. Rev. Lett. **75**, 2432 (1995).
[9] S. Cocco, R. Monasson, and R. Zecchina, Phys. Rev. E **54**, 717 (1996).
[10] A. Engel and M. Weigt, Phys. Rev. E **53**, R2064 (1996).
[11] U. Frisch and G. Parisi, in *Turbulence and Predictability in Geophysical Fluid Dynamics and Climate Dynamics*, edited by M. Ghil, R. Benzi, and G. Parisi (North Holland, Amsterdam, 1985).
[12] T. C. Halsey, M. H. Jensen, L. P. Kadanoff, I. Procaccia, and B. I. Shraiman, Phys. Rev. A **33**, 1141 (1986).
[13] G. Parisi and M. A. Virasoro, J. Phys. (Paris) **50**, 3317 (1989).
[14] M. Biehl and M. Opper, in *Neural Networks: The Statistical Mechanics Perspective*, edited by Jong-Houn Oh, Chulan Kwon, and Sungzoon Cho (World Scientific, Singapore, 1995).
[15] G. Györgyi and N. Tishby, in *Workshop on Neural Networks and Spin Glasses*, edited by K. Theumann and W. K. Koeberle (World Scientific, Singapore, 1990).
[16] M. Opper and D. Haussler, Phys. Rev. Lett. **66**, 2677 (1991).
[17] M. Mezard, G. Parisi, and M. A. Virasoro, *Spin Glass Theory and Beyond* (World Scientific, Singapore, 1987).
[18] V. N. Vapnik and A.Y. Chervonenkis, Theor. Prob. Appl. **16**, 264 (1971).
[19] A. Engel, Mod. Phys. Lett. B **8**, 1683 (1994).
[20] The simplest case is given by a pattern set in which one pattern occurs at least twice since it is, of course, impossible to map identical patterns to different outputs.
[21] T. Bohr and T. Tél, in *Directions in Chaos*, edited by Hao-Bai-Lin (World Scientific, Singapore, 1988).
[22] J. R. L. de Almeida and D. Thouless, J. Phys. A **11**, 983 (1978).
[23] T. Temesvari, C. De Dominicis, and I. Kondor, J. Phys. A **27**, 7569 (1994).
[24] D. Sherrington, and S. Kirkpatrick, Phys. Rev. Lett. **35**, 1972 (1975).
[25] A nonzero external field for the SK model corresponds to a threshold $\sigma = \mathrm{sgn}(\mathbf{J}\cdot\boldsymbol{\xi} - \theta)$ in Eq. (1) breaking explicitly the symmetry giving rise to $Q_0 = 0$. Again similar to the SK model the two instabilities are then expected to separate from each other and a full AT line will show up in the q-θ plane.
[26] W. Krauth and M. Mezard, J. Phys. France **50**, 3057 (1989).
[27] G. Györgyi, Phys. Rev. Lett. **64**, 2957 (1990).
[28] St. Mertens, J. Phys. A **29**, L199 (1996).
[29] St. Mertens and A. Engel, Phys. Rev. E (to be published).
[30] Stambke, diploma thesis, University of Giessen, 1992 (unpublished).
[31] W. Krauth and M. Opper, J. Phys. A **22**, L519 (1989).
[32] W. H. Press, S. A. Teukolsky, W. T. Vetterling, and B. P. Flannery, *Numerical Recipes in C*, 2nd ed. (Cambridge University Press, Cambridge, 1992).